

JET-P(92)61

J.P. Coad, L. de Kock, A. Koch, F. Weschenfelder, P. Wienhold,
R. Wilhelm and JET Team

Assessment Techniques for Measurement of Target Erosion/Redeposition in Large Tokamaks

“This document contains JET information in a form not yet suitable for publication. The report has been prepared primarily for discussion and information within the JET Project and the Associations. It must not be quoted in publications or in Abstract Journals. External distribution requires approval from the Publications Officer, JET Joint Undertaking, Abingdon, Oxon, OX14 3EA, UK”.

“Enquiries about Copyright and reproduction should be addressed to the Publications Officer, EFDA, Culham Science Centre, Abingdon, Oxon, OX14 3DB, UK.”

The contents of this preprint and all other JET EFDA Preprints and Conference Papers are available to view online free at www.iop.org/Jet. This site has full search facilities and e-mail alert options. The diagrams contained within the PDFs on this site are hyperlinked from the year 1996 onwards.

Assessment Techniques for Measurement of Target Erosion/ Redeposition in Large Tokamaks

J.P. Coad, L. de Kock, A. Koch¹, F. Weschenfelder², P. Wienhold²,
R. Wilhelm¹ and JET Team*

JET-Joint Undertaking, Culham Science Centre, OX14 3DB, Abingdon, UK

¹*Max-Planck Institut für Plasmaphysik, W-8046 Garching bei München, Germany*

²*Forschungszentrum Jülich GmbH, W-5170 Jülich, Germany*

** See Annex*

ASSESSMENT TECHNIQUES FOR MEASUREMENT OF TARGET EROSION/REDEPOSITION IN LARGE TOKAMAKS

J P Coad, L de Kock, A Koch*, F Weschenfelder+,
P Wienhold+ and R Wilhelm*

JET Joint Undertaking, Abingdon, Oxon, OX14 3EA, UK

* Max-Planck Institut für Plasmaphysik, W-8046 Garching bei München, FRG

+ Forschungszentrum Jülich GmbH, W-5170 Jülich, FRG

Abstract

Two possible techniques for the measurement of erosion/redeposition in the new JET divertor have been assessed; colour fringe analysis (CFA) and speckle interferometry. CFA is a simple technique in which the target is viewed with a colour camera, and can study deposited films up to $1\mu\text{m}$ in thickness. Speckle interferometry is a powerful technique for following changes in surface topology, but its sensitivity of $> 1\mu\text{m}$ makes it more ideally suited to the next generation of tokamaks.

Introduction

One of the crucial physics issues to be faced in a fusion reactor such as the proposed International Thermonuclear Experimental Reactor (ITER) concerns the amount of power incident at the divertor strike point ⁽¹⁾. Peak power fluxes onto the plasma-facing surfaces during normal operation are expected to be 5-100 MW/m², and much higher during transient events such as disruptions. Extrapolation of the results from existing tokamaks would suggest that at these power levels the rate of erosion by sputtering on the target plates would be unacceptably high. However, if the divertor operates in a high-recycling regime, (i.e. at high target density) local redeposition of the eroded material ⁽²⁾ may reduce the nett erosion to an acceptable level ⁽¹⁾. At the present time these high-recycling conditions cannot be produced reliably so the extent of the redeposition predicted cannot be measured. The Joint European Torus (JET) is currently being re-configured to include a divertor ⁽³⁾ which is planned to operate at conditions close enough to those of ITER for significant local redeposition to be expected. In order to validate the redeposition theory and thus increase

confidence in the probable success of a machine like ITER, it is clearly important to measure the net erosion rate at the new JET divertor target as a function of target density.

Post mortem measurements of the JET divertor targets will be made during and after the first divertor phase (when the target consists of tiles fastened to a rigid support structure). These measurements may give an overall average for the amount of erosion per pulse, but the plasma conditions will have varied considerably, and will not have been close to the ITER parameters. During the second phase, plasma conditions in the divertor should approach those expected for ITER, but the integral cooled target structure will make physical measurements of erosion almost impossible. It is then necessary to identify methods of making time-resolved in-situ (but non-intrusive) measurements of divertor erosion (and deposition in other areas). Two such methods are described in this paper, "Colour Fringe Analysis" and "Speckle Interferometry". The techniques both involve optical viewing of the divertor target, and will be shown to be complementary in several ways, most notably in the amount of erosion/deposition observable.

Experimental: Development of Colour Fringe Analysis

When a thin transparent film is present on a metal or graphite substrate of different optical properties and is viewed in white light, interference colours can be seen. As the film thickness increases colours change through yellow, purple, blue, back to metallic white and then the sequence is repeated with green instead of metallic. Each interference order represents approximately 50 - 200 nm change in film thickness, depending on the optical properties of the film (and substrate). The phenomenon has been used by Wienhold and co-workers for a-C:H and a-C/B:H films deposited in the TEXTOR tokamak to map film thickness (4, 5). Similar deposits on polished substrates were used to determine the optical properties of the films, and to determine a colour/film thickness calibration. The colours of limiter and wall components removed from TEXTOR were then compared with the calibration chart to produce (by hand) contour maps of the samples (6).

The first stage of the development of colour fringe analysis for JET, was to arrange satisfactory in situ viewing of the target in a tokamak. A cross

section of the TEXTOR tokamak is shown in Figure 1. Samples on the movable limiter assembly in TEXTOR were viewed with a colour video camera which was mounted on port A. Lamps of various types were fitted to ports B, C and D. The distances of ports A to D from the target are each about 1.6 m. The samples used were part of a graphite limiter head and an aluminium foil, each with a clear set of coloured fringes from previous experiments. A 50 W lamp with a back-reflector gave adequate illumination from any of ports B, C and D. In practice port D was most satisfactory, because lines of sight from ports B and C to the target were largely blocked by support structures for the ICRH antenna inside the vessel. For incidence at 15° to horizontal from port D using the directed 50 W lamp and a 38 mm camera lens, optimum viewing of the fringes on either sample required an aperture of $f/4$. For illumination from close to the camera, the preferred aperture was $f/5.6$. The distances involved at JET are three times greater, so stronger illumination (which need only last for the 20 msec of a video frame) and more aperture should be able to counteract the order of magnitude reduction in solid angle.

a-C:H films have excellent optical properties for colour fringe analysis. JET currently uses a mixture of beryllium and carbon first wall components, and this is expected to also be the case for the divertor phases (3). As a result, films deposited in the scrape-off-layer (SOL) of JET are normally a mixture of carbon, beryllium and hydrogen isotopes (particularly deuterium) (plus trace impurities) so may be termed a-Be/C:H films. In order to check the optical properties of these films a special probe was exposed in the JET SOL using the Fast Transfer System (FTS) (7). The cylindrical probes consist of an outer (graphite) shield with a longitudinal slot which exposes a sector of the (rotatable) inner collector assembly: a cross-section of the probe is shown in Figure 2. For this experiment the collector was fitted with three sets of nickel and polished silicon samples, and each set of silicon samples had a close-fitting stainless steel shield overlapping one edge. The set of samples being exposed covers a distance of 39 mm through the SOL, which should give a factor of 7 - 10 in film thickness. The first set were exposed to JET pulses 26813 to 26817, whilst the second set were exposed closer to the plasma boundary to the six pulses 26952 to 26957 (a total of 245 secs of 2 MA flat top). Strongly coloured fringes were observed on both sets of samples and the substrate (Si, Ni or stainless steel) did not appear to influence the colours. Colours on the first set ranged through the first order of

interference to yellow of second order, whilst on the second set five orders of interference could be seen.

Ellipsometry data were obtained from the samples of the first set, and the thinnest parts of the second set, but other surfaces were too rough for ellipsometry, possibly due to buckling at the film/substrate interface. The results give a refractive constant of about 1.4 and very low absorption. The refractive constant is remarkably low (cf. 2.2 - 2.4 for a-C:H films), so indicates somewhat thicker films than a-C:H films of the same colour, and leads to the colour-thickness calibration curve on an RGB (red, green, blue) colour plot shown in Figure 3. (Only four basic colours are indicated in the figure, but in practice a large number of hues can be ascribed). Profilometer data taken across the sharp film edges produced by the stainless steel guards, and the results of Ion beam analysis of the samples were both in reasonable agreement with the ellipsometer predictions.

We thus have a preliminary calibration for coloured images from the JET divertor phase if a Be divertor target is installed. Since the calibration relies on only one experiment (and in view of the unusual value for the dielectric constant obtained), a number of polished samples will be installed in JET during its next operational phase, which on retrieval can be used to produce a more definitive calibration curve. The interference colours in the image recorded from the divertor each represent a point in the RGB plot in Figure 3. After an interactive programme to establish interference order, the conversion to thickness can be made automatically using the preprogrammed ellipsometer results. The technique should provide film thicknesses from ~60 nm to ~1 μ m with a sensitivity of about 20 nm.

Experimental: Development of Speckle Interferometry

Conventional interferometry requires a highly reflective surface, and analysis of the specularly - reflected beam. The nature and geometry of the JET divertor makes this technique almost impossible, but the restrictions do not apply to speckle interferometry. A characteristic speckle pattern from a surface illuminated by a laser beam can be obtained at any non-specular observation point near the image plane. The surface can be of any finish and of any material. If a laser operating at two wavelengths is used, superposition of the two speckle patterns leads to a fringe pattern, the shape

and spacing of the fringes depending only on the focusing conditions and the relative wavelengths. Preliminary experiments have been conducted using the strongest lines from a 100 mW Ar ion continuously working (CW) laser at 514.5 nm and 488 nm. The laser and optical components need to be on a rigid bench, but the target can be decoupled from this structure: initial setting up was done using the lid of a tin can. The distance from the final lens to the target, and from the target to the imaging plane was about 50 cm. Observation of the fringes was by a standard CCD camera, and the image could be read into an image processing package on a personal computer.

Figure 4a shows a set of fringes from an area of surface of 5 mm diameter (the laser beam diameter). The inter-fringe spacing, Λ , is given by⁽⁸⁾

$$\Lambda = \frac{\lambda_1 \lambda_2}{(\lambda_1 - \lambda_2)(1 + \cos \theta)}$$

where λ_1 and λ_2 are the two interfering wavelengths and θ is the angle between the laser beam and the surface normal. For the wavelengths quoted above, $\Lambda = 4.7 \mu\text{m}$. Figure 4b shows the effect of viewing across the edge of an ink film on a relatively smooth metal surface (which gives less speckle contrast than in Figure 4a): the film thickness is about $4 \mu\text{m}$. Reasonable values for the limit of detection and the sensitivity of the method are each $1 \mu\text{m}$, but by selecting different wavelengths and interference conditions (e.g. density of the fringes) the upper limit to changes in surface position can be increased to hundreds of microns. Note that changes within the field of view may be positive and/or negative (i.e. erosion and/or deposition).

Further experiments are necessary before speckle interferometry might be applied to JET. The sensitivity range for the technique, and its applicability to technological surfaces such as a divertor element have been demonstrated, but a different laser and a different detection system would be necessary to accommodate the much larger working distance ($\times 10$) required for JET. There is, however, little doubt that similar images would then be obtained over the larger distance. Part of these follow-up experiments would demonstrate imaging larger areas of the target (e.g. 20 - 30 mm diameter to cover a complete divertor element width (3)), and investigate

multiple beam arrays to give imaging of several adjacent areas to give a complete picture of the divertor erosion/redeposition.

Discussion

The first issue to address is the extent of erosion/redeposition expected in the JET divertor. The particle flux and likely incident ion energies for a 4 sec pulse of 20 MW swept over a 20 cm strike zone suggest sputtering losses (without prompt redeposition) of the order of 0.5 to $1\mu\text{m}$ per pulse, which is about a factor of 5 less than the cumulative evaporation expected if water cooled beryllium-faced divertor elements are used ⁽⁹⁾. A schematic of the toroidal cross-section of some divertor elements is shown in Figure 5. The design, wherein each element shields the edge of the adjacent one guarantees that erosion will not be uniform. The flux density for the areas being eroded will be almost twice the toroidal mean and each element will have a region which is not directly exposed and will probably be an area of nett deposition. The topographical contrast across each element will thus be rather larger than the figures above suggest (and would be an ideal field of view for speckle interferometry, subject to the sensitivity limit). These conditions will be reached during the second divertor phase, beginning late 1994. In the first phase beginning late 1993 the divertor will not be directly cooled, and lower fluxes and shorter pulse times will mean losses by sputtering of probably no more than $0.1\mu\text{m}$ per pulse.

Erosion losses from sections of the divertor imply equal (integrated) amounts of deposition elsewhere in the machine (and mostly in other parts of the divertor channel). Deposition rates may approach the peak erosion rates in localised areas but will decrease away from the strike zones (deeper into the SOL) to cover a range of at least two orders of magnitude. Colour fringe analysis can be applied directly to redeposited films, and the magnitude of the deposition expected in the divertor seems to be ideally suited to the method. A direct measure of the erosion rate could be obtained if the thinning of a pre-existing film over the erosion zone were observed. Such a film could, perhaps, be deposited in a previous pulse using different plasma parameters or a gas (e.g. methane) puff near the area observed, or could be present when the divertor was installed.

Deformations of the target will also be detected by speckle interferometry. In order to separate this from erosion/deposition reference surfaces can be used which show no erosion/deposition. Another method could be to use the different time scales to separate the two effects.

The predicted erosion/deposition rates for the first divertor phase are not large enough for speckle interferometry. The intention is to continue the development of the method for application to a tokamak, and to see what erosion actually occurs in the first divertor phase. The results from the first phase will allow an accurate forecast for the second divertor phase, and if this suggests that surface changes per pulse will be visible using speckle interferometry then the technique will be considered as an additional diagnostic for the second phase.

It should be noted that the sensitivity ranges for speckle interferometry and colour fringe analysis do not overlap, the former being able to observe changes $>1 \mu\text{m}$ and the latter $\leq 1 \mu\text{m}$: the techniques may thus be considered to be complementary. If erosion of $1 \mu\text{m}$ per pulse is observed (and speckle interferometry is possible), then the colour fringe analysis will be possible only of deposits in the SOL where rates are much lower. As deposition builds up to $>1 \mu\text{m}$ in a given region or if temperatures regularly exceed 500°C and the optical properties deteriorate, colour fringe analysis will in any case no longer be possible from that area.

Conclusions

Erosion at the divertor has been identified as a major physics issue for the next generation of tokamaks (e.g. ITER), though theory suggests prompt redeposition may mitigate the effect. The new JET divertor should approach ITER conditions and attempts should be made to measure erosion therein.

Colour fringe analysis has been shown to be possible in TEXTOR and to be suitable for a-Be/C:H films. The technique will be used to make in situ measurements of deposition (and possibly erosion of preformed films) routinely in TEXTOR and in JET: the method is applicable to films up to $1 \mu\text{m}$ thick. Speckle interferometry is being developed as a method to measure surface changes of $>1 \mu\text{m}$ in a tokamak. If results from the first

divertor phase of JET suggest erosion per pulse in the second phase may exceed this value for high power shots, it might be possible to include speckle interferometry as a JET diagnostic for the second divertor phase.

References

1. S.A. Cohen, R.F. Mattas and K.A. Werley, Princeton Plasma Physics Lab. report PPPL - 2823, (Feb. 1992) (available from National Technical Information Service, Springfield, Va 22161, USA).
M.F.A. Harrison and E.S. Hotston, J. Nuclear Materials 176-177 (1990) 256.
2. J. Brooks, J. Nuclear Materials 170 (1990) 164.
3. M. Huguet, H. Altmann et al., Proc. 14th Symposium on Fusion Engineering, San Diego, USA, Sept 1991.
4. P. Wienhold and U. Littmark, E-MRS Meeting, June 1987, Vol. XVII, 441 (J. de Physique 1987)
5. F. Weschenfelder, P. Wienhold and J. Winter, 10th Conf. on Plasma Surface Interactions, Monterey, USA, March 1992 (to be published in J. Nuclear Materials).
6. P. Wienfold, F. Waelbroeck, H. Bergsaker, J. Winter and H-G Esser
J. Nuclear Materials 162 - 164 (1989) 369
7. J.P. Coad, J.C.B. Simpson and G.F. Neill, Surface and Interface Analysis 14 (1989) 543.
8. R Jones and C Wykes, "Holographic and Speckle Interferometry" (second edition) Cambridge Studies in Modern Optics : 6, Cambridge University Press (1989).
9. E.B. Deksnis, Private Communication (1992).

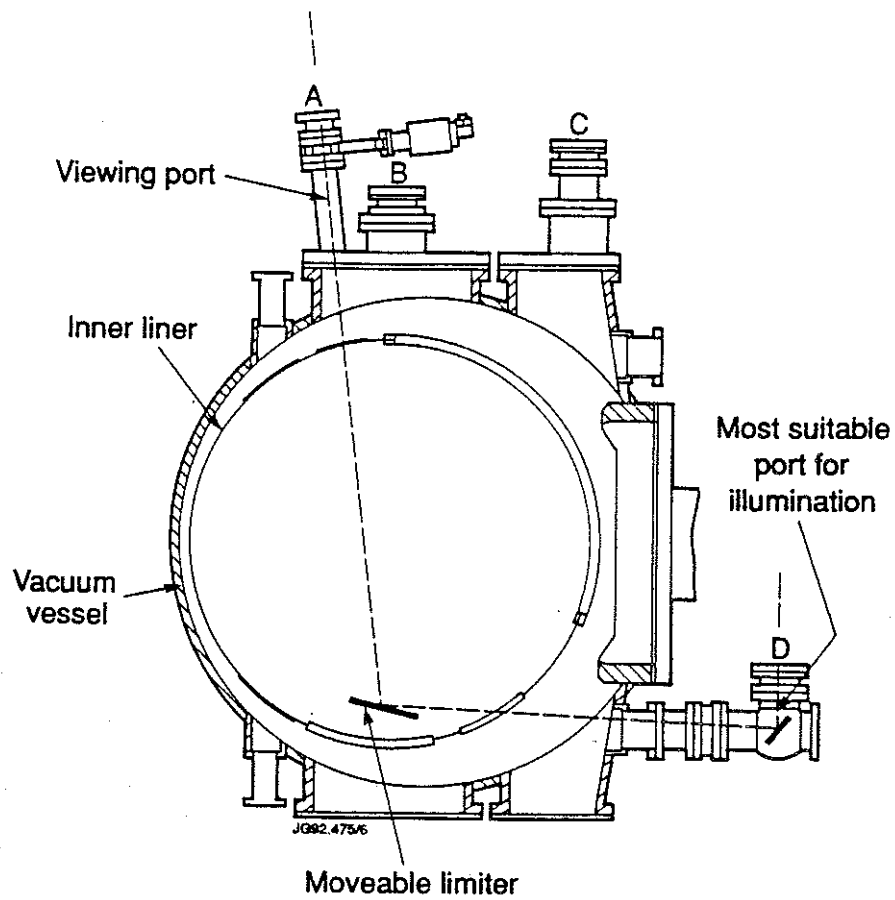


Figure 1 Poloidal cross-section of the TEXTOR tokamak.

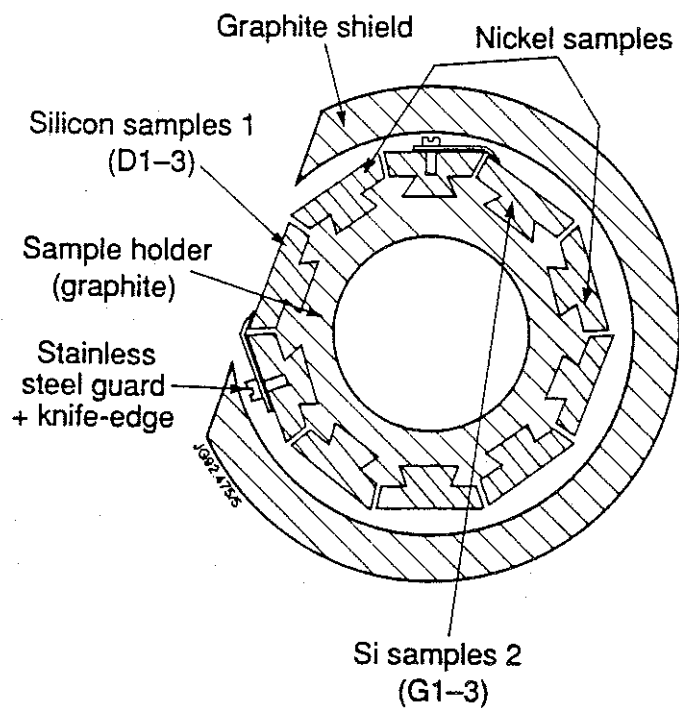


Figure 2 Cross-section of the special probe exposed in JET to provide a reference film of a-Be/C:H

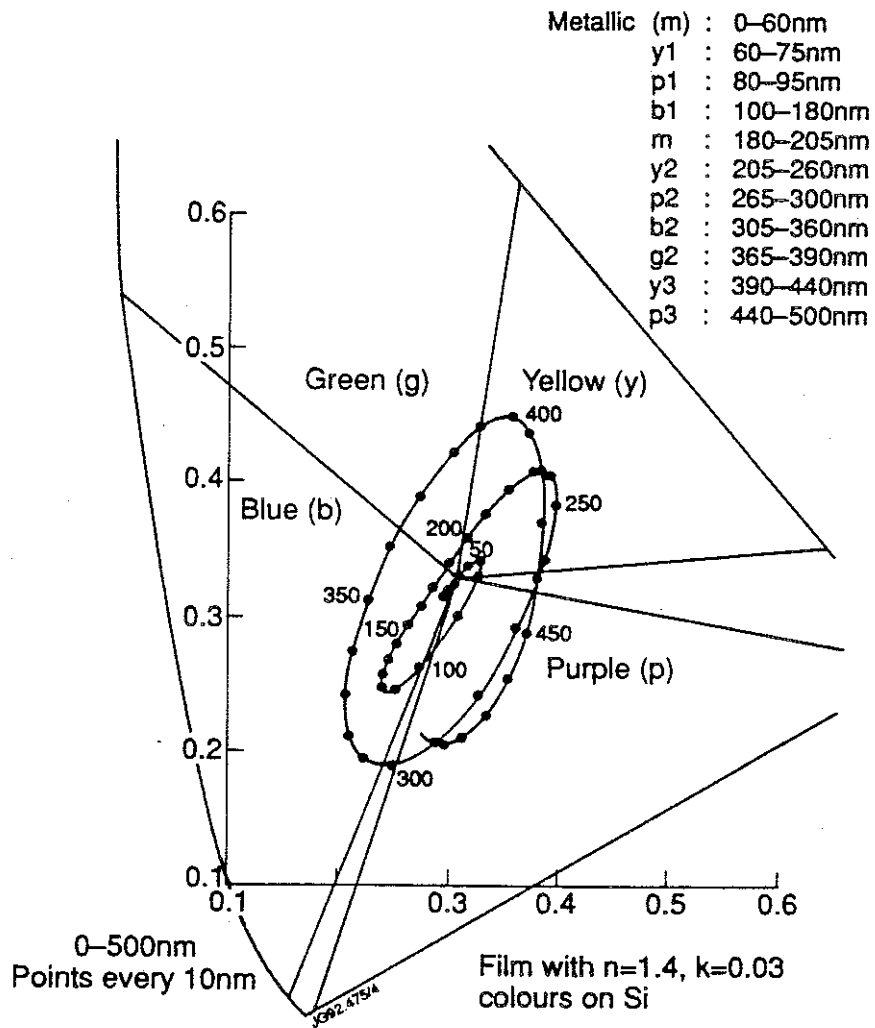


Figure 3 Calibration curve for a-Be/C:H film thickness versus colour (in the RGB coordinate system) based on ellipsometer data

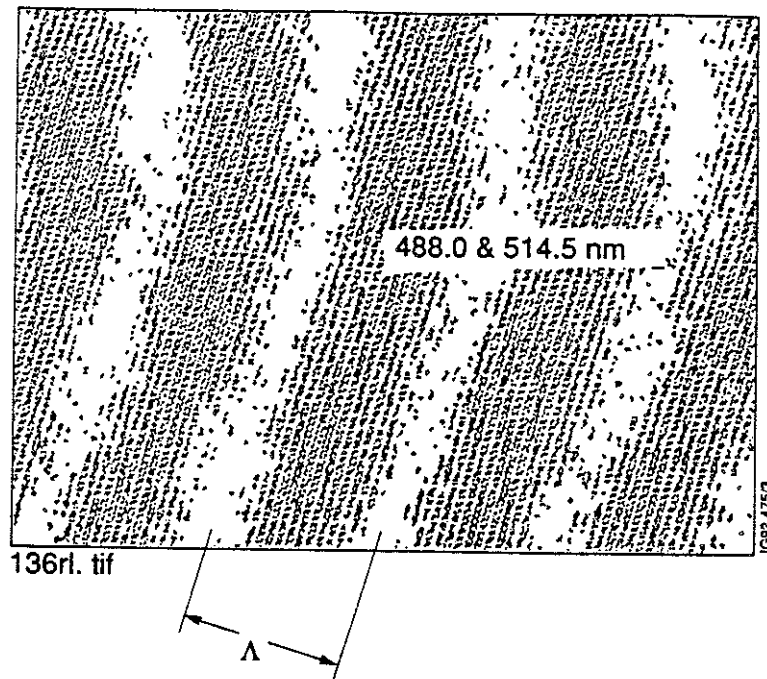
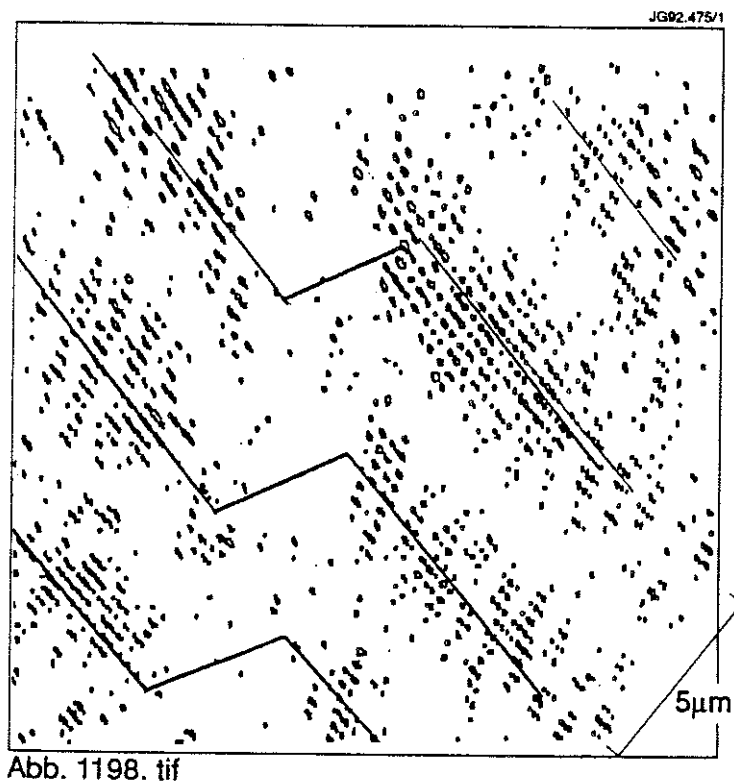


Figure 4(a) The fringe pattern obtained by speckle interferometry from a flat (but unpolished) surface using two laser wavelengths.



(b) The fringe pattern from a 5 mm diameter area including a step of about 4 μm on an otherwise flat surface.

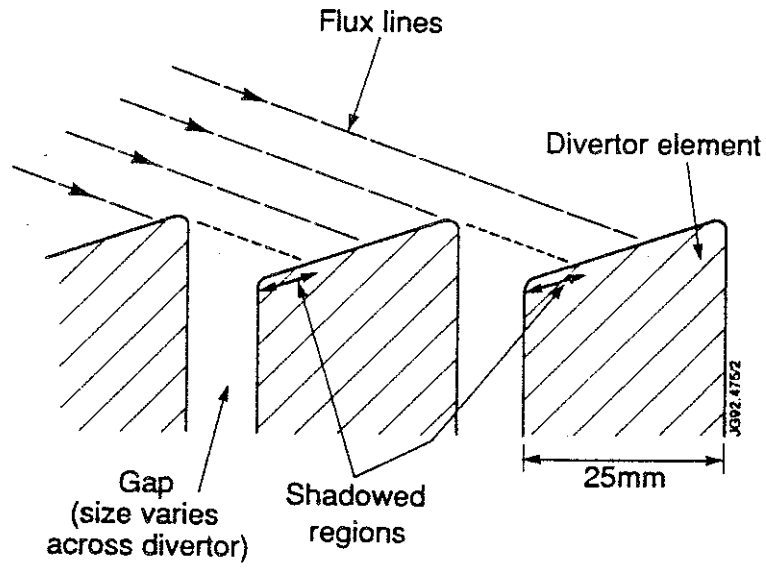


Figure 5 Toroidal cross-section (schematic) of three elements of the proposed JET divertor target. (vertical scale exaggerated)

Appendix I

THE JET TEAM

JET Joint Undertaking, Abingdon, Oxon, OX14 3EA, U.K.

J.M. Adams¹, B. Alper, H. Altmann, A. Andersen¹⁴, P. Andrew, S. Ali-Arshad, W. Bailey, B. Balet, P. Barabaschi, Y. Baranov, P. Barker, R. Barnsley², M. Baronian, D.V. Bartlett, A.C. B  ll, G. Benali, P. Bertoldi, E. Bertolini, V. Bhatnagar, A.J. Bickley, D. Bond, T. Bonicelli, S.J. Booth, G. Bosia, M. Botman, D. Boucher, P. Boucquey, M. Brandon, P. Breger, H. Brelen, W.J. Brewerton, H. Brinkschulte, T. Brown, M. Brusati, T. Budd, M. Bures, P. Burton, T. Businaro, P. Butcher, H. Buttgerreit, C. Caldwell-Nichols, D.J. Campbell, D. Campling, P. Card, G. Celentano, C.D. Challis, A.V. Chankin²³, A. Cherubini, D. Chiron, J. Christiansen, P. Chuilon, R. Claesen, S. Clement, E. Clipsham, J.P. Coad, I.H. Coffey²⁴, A. Colton, M. Comiskey⁴, S. Conroy, M. Cooke, S. Cooper, J.G. Cordey, W. Core, G. Corrigan, S. Corti, A.E. Costley, G. Cottrell, M. Cox⁷, P. Crawley, O. Da Costa, N. Davies, S.J. Davies⁷, H. de Blank, H. de Esch, L. de Kock, E. Deksnis, N. Deliyanakus, G.B. Denne-Hinnov, G. Deschamps, W.J. Dickson¹⁹, K.J. Dietz, A. Dines, S.L. Dmitrenko, M. Dmitrieva²⁵, J. Dobbing, N. Dolgetta, S.E. Dorling, P.G. Doyle, D.F. D  chs, H. Duquenoy, A. Edwards, J. Ehrenberg, A. Ekedahl, T. Elevant¹¹, S.K. Erents⁷, L.G. Eriksson, H. Fajemirokun¹², H. Falter, J. Freiling¹⁵, C. Froger, P. Froissard, K. Fullard, M. Gadeberg, A. Galetsas, L. Galbiati, D. Gambier, M. Garribba, P. Gaze, R. Giannella, A. Gibson, R.D. Gill, A. Girard, A. Gondhalekar, D. Goodall⁷, C. Gormezano, N.A. Gottardi, C. Gowers, B.J. Green, R. Haange, A. Haigh, C.J. Hancock, P.J. Harbour, N.C. Hawkes⁷, N.P. Hawkes¹, P. Haynes⁷, J.L. Hemmerich, T. Hender⁷, J. Hoekzema, L. Horton, J. How, P.J. Howarth⁵, M. Huart, T.P. Hughes⁴, M. Huguet, F. Hurd, K. Ida¹⁸, B. Ingram, M. Irving, J. Jacquinet, H. Jaeckel, J.F. Jaeger, G. Janeschitz, Z. Jankowicz²², O.N. Jarvis, F. Jensen, E.M. Jones, L.P.D.F. Jones, T.T.C. Jones, J-F. Junger, F. Junique, A. Kaye, B.E. Keen, M. Keilhacker, W. Kerner, N.J. Kidd, R. Konig, A. Konstantellos, P. Kupschus, R. L  sser, J.R. Last, B. Laundry, L. Lauro-Taroni, K. Lawson⁷, M. Lennholm, J. Lingertat¹³, R.N. Litunovski, A. Loarte, R. Lobel, P. Lomas, M. Loughlin, C. Lowry, A.C. Maas¹⁵, B. Macklin, C.F. Maggi¹⁶, G. Magyar, V. Marchese, F. Marcus, J. Mart, D. Martin, E. Martin, R. Martin-Solis⁸, P. Massmann, G. Matthews, H. McBryan, G. McCracken⁷, P. Meriguet, P. Miele, S.F. Mills, P. Millward, E. Minardi¹⁶, R. Mohanti¹⁷, P.L. Mondino, A. Montvai³, P. Morgan, H. Morsi, G. Murphy, F. Nave²⁷, S. Neudatchin²³, G. Newbert, M. Newman, P. Nielsen, P. Noll, W. Obert, D. O'Brien, J. O'Rourke, R. Ostrom, M. Ottaviani, S. Papastergiou, D. Pasini, B. Patel, A. Peacock, N. Peacock⁷, R.J.M. Pearce, D. Pearson¹², J.F. Peng²⁶, R. Pepe de Silva, G. Perinic, C. Perry, M.A. Pick, J. Plancoulaine, J-P. Poff  , R. Pohlchen, F. Porcelli, L. Porte¹⁹, R. Prentice, S. Puppin, S. Putvinskii²³, G. Radford⁹, T. Raimondi, M.C. Ramos de Andrade, M. Rapisarda²⁹, P-H. Rebut, R. Reichle, S. Richards, E. Righi, F. Rimini, A. Rolfe, R.T. Ross, L. Rossi, R. Russ, H.C. Sack, G. Sadler, G. Saibene, J.L. Salanave, G. Sanazzaro, A. Santagiustina, R. Sartori, C. Sborchia, P. Schild, M. Schmid, G. Schmidt⁶, H. Schroepf, B. Schunke, S.M. Scott, A. Sibley, R. Simonini, A.C.C. Sips, P. Smeulders, R. Smith, M. Stamp, P. Stangeby²⁰, D.F. Start, C.A. Steed, D. Stork, P.E. Stott, P. Stubberfield, D. Summers, H. Summers¹⁹, L. Svensson, J.A. Tagle²¹, A. Tanga, A. Taroni, C. Terella, A. Tesini, P.R. Thomas, E. Thompson, K. Thomsen, P. Trevalion, B. Tubbing, F. Tibone, H. van der Beken, G. Vlases, M. von Hellermann, T. Wade, C. Walker, D. Ward, M.L. Watkins, M.J. Watson, S. Weber¹⁰, J. Wesson, T.J. Wijnands, J. Wilks, D. Wilson, T. Winkel, R. Wolf, D. Wong, C. Woodward, M. Wykes, I.D. Young, L. Zannelli, A. Zolfaghari²⁸, G. Zullo, W. Zwingmann.

PERMANENT ADDRESSES

1. UKAEA, Harwell, Didcot, Oxon, UK.
2. University of Leicester, Leicester, UK.
3. Central Research Institute for Physics, Budapest, Hungary.
4. University of Essex, Colchester, UK.
5. University of Birmingham, Birmingham, UK.
6. Princeton Plasma Physics Laboratory, New Jersey, USA.
7. UKAEA Culham Laboratory, Abingdon, Oxon, UK.
8. Universidad Complutense de Madrid, Spain.
9. Institute of Mathematics, University of Oxford, UK.
10. Freien Universit  t, Berlin, F.R.G.
11. Royal Institute of Technology, Stockholm, Sweden.
12. Imperial College, University of London, UK.
13. Max Planck Institut f  r Plasmaphysik, Garching, FRG.
14. Ris   National Laboratory, Denmark.
15. FOM Instituut voor Plasmafysica, Nieuwegein, The Netherlands.
16. Dipartimento di Fisica, University of Milan, Milano, Italy.
17. North Carolina State University, Raleigh, NC, USA
18. National Institute for Fusion Science, Nagoya, Japan.
19. University of Strathclyde, 107 Rottenrow, Glasgow, UK.
20. Institute for Aerospace Studies, University of Toronto, Ontario, Canada.
21. CIEMAT, Madrid, Spain.
22. Institute for Nuclear Studies, Otwock-Swierk, Poland.
23. Kurchatov Institute of Atomic Energy, Moscow, USSR
24. Queens University, Belfast, UK.
25. Keldysh Institute of Applied Mathematics, Moscow, USSR.
26. Institute of Plasma Physics, Academica Sinica, Hefei, P. R. China.
27. LNETI, Savacem, Portugal.
28. Plasma Fusion Center, M.I.T., Boston, USA.
29. ENEA, Frascati, Italy.